Proc. Natl. Acad. Sci. USA
Vol. 95, pp. 15112–15117, December 1998
Plant Biology

The *Arabidopsis thaliana AGRAVITROPIC 1* gene encodes a component of the polar-auxin-transport efflux carrier

RUJIN CHEN*†, PIERRE HILSON*†‡, JOHN SEDBROOK*, ELIZABETH ROSEN*, TIMOTHY CASPAR§, AND PATRICK H. MASSON*¶

*Laboratory of Genetics, University of Wisconsin, 445 Henry Mall, Madison, WI 53706; and §Central Research and Development, Experimental Research Station, E.I. DuPont de Nemours and Co., Wilmington, DE 19880-0402

Communicated by Nina Fedoroff, Pennsylvania State University, University Park, PA, October 15, 1998 (received for review September 24, 1998)

ABSTRACT **Auxins are plant hormones that mediate many aspects of plant growth and development. In higher plants, auxins are polarly transported from sites of synthesis in the shoot apex to their sites of action in the basal regions of shoots and in roots. Polar auxin transport is an important aspect of auxin functions and is mediated by cellular influx and efflux carriers. Little is known about the molecular identity of its regulatory component, the efflux carrier [Estelle, M. (1996) *Current Biol.* 6, 1589–1591]. Here we show that mutations in the *Arabidopsis thaliana AGRAVITROPIC 1* (*AGR1*) gene involved in root gravitropism confer increased root-growth sensitivity to auxin and decreased sensitivity to ethylene and an auxin transport inhibitor, and cause retention of exogenously added auxin in root tip cells. We used positional cloning to show that *AGR1* encodes a putative transmembrane protein whose amino acid sequence shares homologies with bacterial transporters. When expressed in *Saccharomyces cerevisiae*, *AGR1* promotes an increased efflux of radiolabeled IAA from the cells and confers increased resistance to fluoro-IAA, a toxic IAA-derived compound. *AGR1* transcripts were localized to the root distal elongation zone, a region undergoing a curvature response upon gravistimulation. We have identified several *AGR1*-related genes in *Arabidopsis*, suggesting a global role of this gene family in the control of auxin-regulated growth and developmental processes.**

Plant roots typically grow downward, at a defined angle from the gravity vector. They respond to deviations from the defined growth angle (gravistimulation) by developing a curvature at the distal and central elongation zones, which eventually allows their tip to resume a normal growth pattern. The gravitropic response involves perception of the gravistimulus by the root cap columella cells, transduction of that physical information into physiological signals, transmission of the signals to the distal and central elongation zones, and curvature response (1). Physiological evidence suggests that auxin and, possibly, apoplastic Ca^{2+} constitute the physiological signals that are transmitted to the root distal and central elongation zones and are responsible for the curvature response (1).

Basipetal transmission of auxin is mediated by polar auxin transport machinery, which involve influx and efflux carriers. The polarity of auxin transport probably is established by a basal localization of the efflux carrier in transporting cells (2). In this report, we demonstrate that the *Arabidopsis thaliana AGR1* gene encodes a component of the auxin efflux carrier that mediates the root gravitropic response.

The publication costs of this article were defrayed in part by page charge payment. This article must therefore be hereby marked "*advertisement*" in accordance with 18 U.S.C. §1734 solely to indicate this fact.

MATERIALS AND METHODS

Plant Stocks. The following alleles were analyzed and found to belong to the same complementation group: *agr1–1*, *agr1–2*, *agr1–3* (Landsberg *erecta*; previously named as *agr-1*, *agr-2*, and *agr-3*, respectively) (3), *agr1–4* (Wassilewskija; WS), *agr1–5*, *agr1–6*, *agr1–7*, and *agr1–8* (Estland), *wav6* (Landsberg; *agr1–52*) (4), and *eir1–1* (Columbia) (5). Manipulation of plant stocks was described previously (6).

Quantification of Root Growth. The rate of root growth was measured (6). Briefly, 4- to 5-day-old seedlings were transplanted onto 0.8% agar-based media containing one-half strength Murashige and Skoog (MS) salts and 1.5% sucrose (Sigma), with or without one of the chemicals described below. They were grown for 48 hr in a growth chamber at 22°C with a photoperiod of 16 hr and a light intensity of 80 μE m^{-2} s^{-1}. Pictures were taken 0, 24, and 48 hr after seedlings were transferred to the test medium. Root length was measured by using an NIH IMAGE analysis program (http://rsb.info.nih.gov/nih-image/). Reported results correspond to the growth rates measured over the 48-hr test period. However, identical results were obtained when growth rates were measured over a 24-hr period (data not shown). 1-Naphthaleneacetic acid (1-NAA), 1-aminocyclopropane-1-carboxylic acid (ACC), and 2,3,5-triiodobenzoic acid (TIBA) were obtained from Sigma and prepared as 10 mM stock solutions in diluted NaOH, 10% isopropanol, and water, respectively (7).

Auxin Efflux Assays. Auxin efflux in root tips was measured using a modification of the procedure described earlier (8). Three-millimeter-long root tips of 20 5-day-old light-grown seedlings were excised and incubated for 2 hr in one-half MS media containing 1.5% sucrose and 3.3×10^{-8} M 3-[5(n)-^{3}H]indolylacetic acid (^{3}H-IAA; 21Ci/mmol; Amersham). Samples were rinsed and incubated for 2 hr in the same media without ^{3}H-IAA. After another rinse, samples were soaked for 18 hr in 5 ml scintillation fluid and amounts of ^{3}H-IAA present in the root tips were measured in a scintillation counter.

Root-Wave Assay. Root waving on a tilted agar surface was examined to assess root gravitropism (4, 6).

Positional Cloning. A mapping population segregating for polymorphic chromosomal markers in the WS and Columbia ecotypes was generated by self-pollination of F1 plants derived from a cross between homozygous *agr1–4* plants (WS) and wild-type Columbia plants. F2 progeny were self-pollinated to

Abbreviations: ACC, 1-aminocyclopropane-1-carboxylic acid; F-IAA, 5-fluoro-1-indole-3-acetic acid; IAA, indole-3-acetic acid; 1-NAA, 1-naphthaleneacetic acid; TIBA, 2,3,5-triiodobenzoic acid; WS, Wassilewskija.

Data deposition: The sequence reported in this paper has been deposited in the GenBank database (accession no. AF087459).

†R.C. and P.H. contributed equally to this work.
‡Present address: Department of Plant Pathology, University of Wisconsin, 1630 Linden Drive, Madison, WI 53706.
¶To whom reprint requests should be addressed at: Laboratory of Genetics (3264), University of Wisconsin, 445 Henry Mall, Madison, WI 53706. e-mail: pmasson@macc.wisc.edu.

generate F3 families. Individual F2 plants were progeny-typed to define their genetic constitution at *AGR1*. Two pools of 22 homozygous wild-type and 22 homozygous mutant F3 families were generated and their genomic DNAs were used in a bulked segregant analysis (9) to identify the *AGR1*-linked *nga129* (10) and *LFY3* (11) cleared amplified polymorphic sequences markers.

To fine-map *AGR1*, two populations of F2 plants segregating for polymorphic chromosomal markers were generated by self-pollination of F1 plants derived from crosses between homozygous *agr1–4* plants (WS ecotype) and transgenic No-*O* lines (12) carrying a *Ds* element either 7 cM proximal to *AGR1* (*Ds*389–14) or 3 cM distal to *AGR1* (*Ds*392–13) (Fig. 2*a*). Individual F3 families were tested for hygromycin resistance (*Ds* marker) (12) and for root gravitropism. Families homozygous for *agr1–4* and hemizygous for *Ds*, or heterozygous for *AGR1* and null for *Ds*, were retained, because each of them carried recombined chromosome 5 with a recombination breakpoint between *Ds* and *AGR1*.

Restriction fragment length polymorphism (RFLP) analysis of these two populations was carried out as described (11). Libraries for genomic lambda (13), cosmid (14), and yeast artificial chromosome (YAC; ref. 15) clones were screened by using standard procedures (16). End-fragment probes were isolated by PCR amplification (16) or by restriction-enzyme digestion.

Plant Transformation. Genomic DNA fragments in a binary cosmid vector (COS3A and COS46A) were introduced into *agr1–1*, *agr1–4*, and *agr1–5* mutants by a vacuum-infiltration transformation procedure (17). Similarly, an *Eco*RI subfragment of COS46A (E25) was inserted into the pBIN19 binary vector and introduced into transgenic *agr1–1* and *agr1–5* plants. Transgenic plants were selected on one-half MS media containing either 20 μg/ml of hygromycin (Sigma) for COS3A and COS46A transformants or 50 μg/ml of kanamycin (Sigma) for E25 transformants. Individual T2 progeny from several independent primary transformants were scored for root-waving and antibiotic-resistance phenotypes, as described (6).

Amplification and Sequencing of Genomic DNA and Full-Length cDNA. Genomic DNA was isolated from *agr1–4*, *agr1–5*, and *agr1–6* mutant and wild-type plants. The corresponding *AGR1* locus was PCR-amplified to generate two overlapping fragments with the following PCR-primer pairs: (*i*) 5′-CTAACACGTTGGTAATGGGAATC-3′ and 5′-TGTCGTGAGGAGGAATAGAAACTT-3′, and (*ii*) 5′-GGAGTCAAGAAAAAGGAAAGTGG-3′ and 5′-CGCAAAACTTATCATCAGCAACTA-3′. PCRs were carried out by using the Elongase enzyme mix, according to the manufacturer's instructions (GIBCO/BRL).

The full-length *AGR1* cDNA was amplified by reverse-transcriptase–PCR, using the following primer pair: 5′-ATGATCACCGGCAAAGACATG-3′ and 5′-CACCTTTGGGTCGTATCGCC-3′, as described (16). The first-strand cDNA was synthesized from 10 μg of total L*er*-root RNA by using a Superscript II RNaseH$^-$ Reverse Transcriptase (GIBCO/BRL) following manufacturer's instructions.

The 7-kb *Bam*HI subfragment of E25 was sequenced by using a shot-gun subcloning and sequencing approach. Genomic fragments containing the coding region of the *agr1–4* allele, or overlapping with deletion breakpoints in *agr1–5* and *agr1–6*, as well as a cDNA fragment containing the alternatively spliced exon of *agr1–4* also were sequenced using a dye terminator cycle sequencing kit (Perkin–Elmer) and an Applied Biosystems sequencer.

A 900-bp-long *AGR1* cDNA clone, containing 600 bp of the coding region, 265 bp of the 3′ untranslated region, and a poly(A) tail, was isolated from a cDNA library (18) using a ^{32}P-labeled E25 probe and sequenced.

Functional Assays in *Saccharomyces cerevisiae*. The pAGR1 and pANTI-AGR1 plasmids were generated by cloning a PCR-amplified full-length *AGR1* cDNA into the *Eco*RI site of p426 GAL1 (19) (ATCC no. 87333), downstream of the GAL promoter, in the sense and antisense orientations, respectively. Both plasmids were introduced into *Saccharomyces cerevisiae* strain W3031A (*MATa, ade2–1, his3–11/15, leu2–3/112, trp1–1, ura3–1, can1–100*) as described (16). Transformants were isolated and grown on synthetic complete medium without uracil, supplemented with 2% glucose (16). Because W3031A[pAGR1] transformants did not grow in the presence of galactose, and because the GAL promoter is expressed at a low level when cells are grown on a glucose-containing medium (19), all experiments were carried out on synthetic complete medium without uracil and supplemented with 2% glucose.

To measure auxin efflux in yeast, overnight-grown cultures of W3031A[pAGR1] and W3031A[pANTI-AGR1] were centrifuged. Cells were washed and diluted in fresh medium and regrown for 10 hr. Cells (2×10^9) were pelleted, washed twice with 10 ml of water, and resuspended in 1 ml of 10 mM Mes-Tris buffer (pH 4.6) containing 2% glucose. After a 15-min preincubation at 30°C, 476 pmol of ^{3}H-IAA (21Ci/mmol; Amersham) was added to each culture and cells were incubated for 20 min before being washed three times with 10 ml ice-cold water, resuspended in 10 ml of 10 mM Mes-Tris buffer (pH 4.6) containing 2% glucose, and incubated at 30°C. One-milliliter aliquots were removed at times 0 and 60 min. Cells were pelleted and resuspended in 100 μl of ice-cold water. Retained radioactive counts were determined by a scintillation counter.

To determine the resistance of transformed cells to 5-fluoro-indole-3-acetic-acid (F-IAA; Sigma), overnight-grown cultures of W3031A[pAGR1] and W3031A[pANTI-AGR1] were diluted in SC growth medium without uracil to a cell density of $OD_{600} = 0.05$. For each strain, five equal aliquots were prepared, and different amounts of this F-IAA stock solution (100 mM in ethanol) were added to reach final concentrations of 0, 0.01, 0.1, 1, and 3 mM, respectively. Cultures were grown at 30°C on a rotating shaker, and ODs were measured with a Milton Roy Spectrophotometer Spectronic 20D immediately after addition of F-IAA (time 0), as well as after 3, 7, 10, and 13 hr of growth. Three independent cultures were subjected to that experimental scheme. At each time point, the average OD was calculated for each culture condition, and a relative growth inhibition ratio was calculated by dividing the average OD difference between the control and the F-IAA-treated cultures by the average OD of the control culture. Three millimolar F-IAA completely inhibited the growth of both transformed cell types, while 0.01 and 0.1 mM F-IAA had no effects on the growth of either cultures (data not shown). Data are shown for cells treated with 1 mM F-IAA.

Northern Blot and Whole-Mount *in Situ* Hybridization Experiments. Total RNA was isolated from plant tissues, electrophoresed, blotted, and hybridized with ^{32}P-labeled probes following standard procedures (16).

Whole-mount *in situ* hybridization experiments on 3-day-old *Arabidopsis* seedlings were carried out as described (17) with the following modifications. A recombinant pZL1 plasmid (GIBCO/BRL) carrying the 900-bp-long *AGR1* cDNA was linearized with either *Sal*I or *Not*I to generate templates for *in vitro* synthesis of digoxigenin-labeled sense or antisense AGR1 RNA probes, following the manufacturer's instructions (Boehringer Mannheim). The RNA probes were hydrolyzed to 150 nt, and 10 ng was used in the hybridization reactions.

RESULTS

***agr1* Mutations Alter Root-Growth Sensitivity to 1-NAA, ACC, and TIBA.** Mutations in the *AGR1* gene were identified and shown to confer specific defects in root gravitropism (3–5) (see *Materials and Methods*). Interestingly, one of these alleles

(*eir1–1*) also was shown to mediate increased root-growth resistance to ethylene (5). The *agr1–3* allele, on the other hand, was reported to confer increased root sensitivity to auxin (3) (see *Materials and Methods*). These observations prompted us to analyze the root-growth response to both auxin and ethylene for plants homozygous for several *agr1* alleles (*agr1–1* to *agr1–8*, *eir1–1*, and *wav6*; see *Materials and Methods*).

Fig. 1*a* shows that the growth of *agr1–5* roots was inhibited more by 0.3 μM 1-NAA than that of wild-type Estland roots. The difference was highly significant (*t* test, $P = 2 \times 10^{-6}$). Both wild-type and *agr1–5* mutant roots grew at comparable rates in the absence of 1-NAA or in the presence of 0.01, 1, and 3 μM 1-NAA ($0.1 < P < 0.8$). An increased root-growth sensitivity to 0.3 μM 1-NAA was observed in plants homozygous for all *agr1* alleles tested (data not shown).

agr1 mutations also caused decreased sensitivity to ACC, a precursor of ethylene biosynthesis. Fig. 1*b* shows that *agr1–5* roots grew faster than wild-type roots in the presence of 1 or 3 μM ACC ($P = 2 \times 10^{-9}$ and 7×10^{-9}, respectively). Plants homozygous for all *agr1* alleles tested exhibited a similar degree of decreased sensitivity to 1 or 3 μM ACC (data not shown).

To test the possible involvement of *AGR1* in the polar transport of auxin in roots, we compared the inhibitory effects of a polar auxin transport inhibitor, TIBA, on wild-type and mutant root growth (see *Materials and Methods*). Results shown in Fig. 1*c* indicate that *agr1–5* mutant roots grew significantly faster than wild-type roots in the presence of 10, 30, or 100 μM TIBA ($P = 7.8 \times 10^{-4}$, 1.9×10^{-5}, and 8.7×10^{-7}, respectively). Mutant root growth was at 1.4–2.5 times the rate of wild-type root growth in the presence of TIBA for *agr1–1, agr1–2, agr1–3, agr1–5, agr1–6, eir1–1,* and *wav6* (data not shown).

***agr1* Mutants Retain More Preloaded ^{3}H-IAA in Their Root Tips than Wild Type.** To identify possible defects in the auxin efflux activity in mutant roots, we measured the retention of preloaded ^{3}H-IAA by wild-type and *agr1–5* mutant root tips. Fig. 1*d* shows that ^{3}H-IAA-pretreated *agr1–5* mutant root tips retained most of the radioactive counts after a 2-hr washing period while wild-type root tips retained only 60% of the counts during that period ($P = 0.1$ for the experiment shown in Fig. 1*d*, and 2×10^{-2} and 2×10^{-4} in two other experiments).

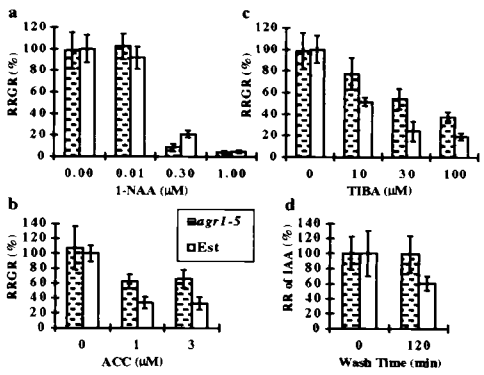

FIG. 1. Physiological analysis of *agr1–5* mutant seedlings. Effects of 1-NAA (*a*), ACC (*b*), and TIBA (*c*) on wild-type and *agr1–5* mutant root growth rates. The average root growth rate of wild-type Estland seedlings in media containing no supplements (12.3 mm for *a* and *c*, and 9.3 mm for *b*) was plotted as 100%. Each data point represents the average of the relative root growth rate (RRGR) for 6–16 wild-type Estland seedlings and for 10–12 *agr1–5* mutant seedlings. (*d*) Relative retention (RR) of ^{3}H-IAA by wild-type and *agr1–5* mutant root tips. The average ^{3}H-IAA retention at time 0 by wild-type and *agr1–5* root tips (4,465 and 3,912 cpm, respectively) was plotted as 100%. Each data point represents the average of three replicates. In *a–d*, the SDs are represented by vertical bars. See *Materials and Methods* for experimental procedures.

***AGR1* Encodes a Putative Transmembrane Protein with Homologies to Bacterial Transporters.** To characterize *AGR1*, we adopted a map-based strategy to clone the locus (Fig. 2*a*). *AGR1* was mapped between the m233 and m558 RFLP markers (20) on chromosome 5 (Fig. 2*a*). Hence, a contig of genomic clones in the form of YACs overlapping with the m558 marker was identified (15) and characterized (Fig. 2*b*). New molecular markers (T21207, T22106, and 10B4L) were identified and ordered along the contig (Fig. 2*b*; *Materials and Methods*). The molecular marker closest to *AGR1* (T22106) then was used as a probe to generate a contig of lambda and cosmid clones (Fig. 2*c*; *Materials and Methods*). Additional RFLP markers were mapped relative to *AGR1* on that contig. 1L and 46L were identified as the closest markers flanking *AGR1* (Fig. 2*c*).

AGR1 was mapped further onto the cosmid COS46A clone by a transformation–rescue approach. When introduced into *agr1–1, agr1–4*, and *agr1–5* plants, COS46A rescued the altered root-wave phenotype associated with the mutations (Fig. 2*d*), while the COS3A clone did not (data not shown). Furthermore, the wild-type root-wave phenotype was found to cosegregate with the presence of the COS46A transgene in the T2 progenies of at least 16 COS46A primary transformants (data not shown). An internal 10-kb *Eco*RI subclone of COS46A (named E25) also was able to rescue the mutant root-wave

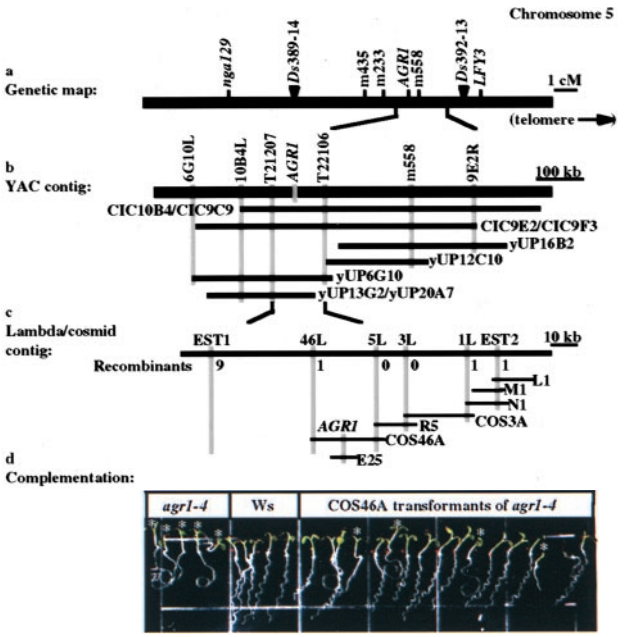

FIG. 2. Genetic and physical maps of the *AGR1* region of chromosome 5. (*a*) Genetic map of the *nga129* and *LFY3* region of chromosome 5, showing the relative genetic positions of the *nga129*, m233, m558, and *LFY3* markers, and the positions of the *Ds* 389–14 and *Ds* 392–13 insertions. (*b*) Mapping of *AGR1* on a YAC contig of cloned genomic DNA fragments, showing the relative positions of specific RFLP markers (drawn as vertical shaded bars) and positions of individual YAC clones (drawn as horizontal black bars). (*c*) Fine mapping of *AGR1* on a contig of cosmid (COS3A and COS46A) and lambda (L1, M1, N1, and R5) genomic clones, showing the number of recombinants identified in the mapping populations (see *Materials and Methods*) with recombination breakpoints between *AGR1* and individual RFLP markers. Scales are in recombination units for *a* or kilobase pairs of DNA for *b* and *c*. (*d*) Wavy root-growth phenotype of segregating F2 plants (*Right*) derived from an *agr1–4* plant (*Left*) transformed with the COS46A clone. Wild-type untransformed control plants are also shown (*Center*). Mutant seedlings are indicated by an asterisk.

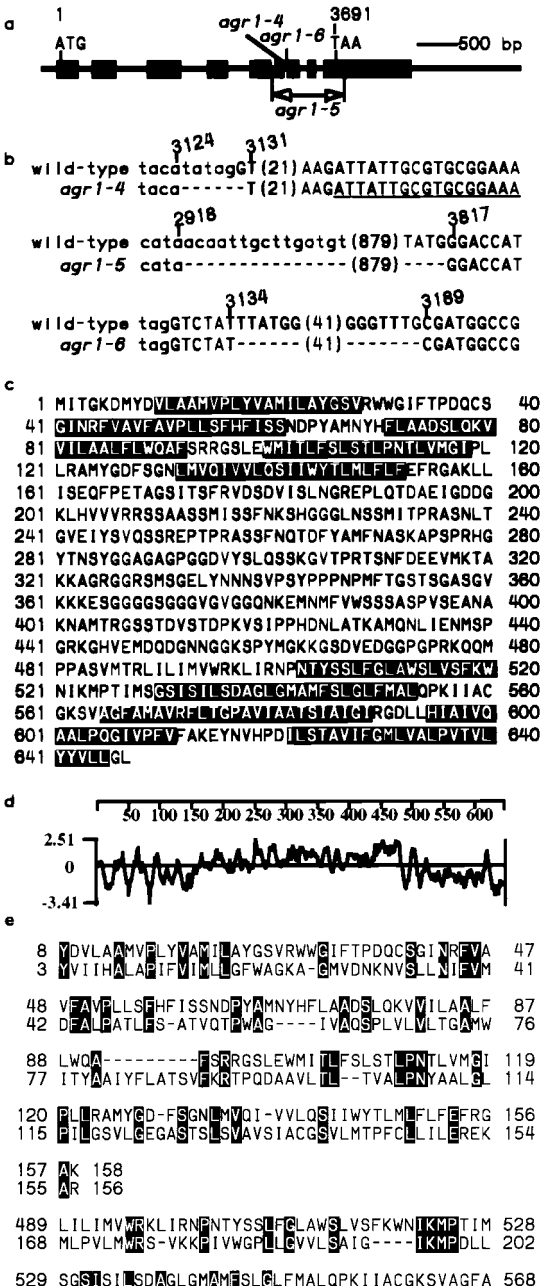

FIG. 3. The *Arabidopsis AGR1* gene. (*a*) The structure of *AGR1*. The exons are shown in solid boxes. The initiation (ATG) and stop (TAA) codons are also shown, with their positions indicated above the nucleotide sequence. The first nucleotide of the initiation codon was arbitrarily chosen as 1. (*b*) Nature of the mutations found in the *agr1–4, agr1–5*, and *agr1–6* alleles. Exon and intron sequences are shown in upper- and lowercase letters, respectively. The exon derived from the alternative splicing of the *agr1–4* transcript is underlined. Deleted nucleotides are represented by dashes. Numbers in parentheses represent nucleotides omitted because of space limitation. (*c*) The amino acid sequence of the AGR1 protein. Predicted transmembrane domains are boxed (22). (*d*) Kyte–Doollitle hydropathy plot of the AGR1 protein sequence. (*e*) Alignment of the amino acid sequences of AGR1 and *Methanococcus* MdcF (24). The AGR1 (top) and the MdcF (bottom) sequences were aligned using the NIH GAPPED BLAST SEARCH program (23). Identical and functionally conserved amino acids are shown in solid and shaded boxes, respectively. Sequence gaps are represented by dashed lines.

phenotype when introduced into *agr1–1* and *agr1–5* mutant plants (data not shown).

A 7-kb *Bam*HI subfragment of E25 was sequenced and a functional gene was predicted (21). The full-length cDNA was cloned and sequenced. As shown in Fig. 3*a*, the E25 gene consists of 9 exons and 8 introns. It encodes a hypothetical protein of 647 aa with a predicted molecular mass of 69 kDa.

A molecular analysis of the E25 gene in *agr1–4*, *agr1–5*, and *agr1–6* plants confirmed its *AGR1* identity (Fig. 3 *a* and *b*). The *agr1–4* allele was found to carry a 6-bp deletion that altered the acceptor splice site of intron 6. Analysis of the corresponding cDNA sequence identified an alternative splicing of the transcribed sequence. Consequently, the *agr1–4* mRNA carried a reading-frame shift and a premature stop codon (Fig. 3*b*). The *agr1–5* allele was shown to carry a 898-bp deletion starting at the middle of the fifth intron and ending 123 bp downstream of the stop codon. As a result, a total of 128 aa should be deleted from the carboxyl end of the putative AGR1 protein, if expressed. The *agr1–6* allele was shown to carry a 54-bp deletion in the seventh exon (Fig. 3*b*), resulting in the removal of 18 aa beginning at position 550 of the protein and the replacement of alanine-568 by serine.

The *agr1–7* and *agr1–8* alleles also were characterized. A deletion spanning the entire *AGR1* locus and at least 0.5 cM of chromosomal DNA distal to the locus was identified in both alleles (data not shown).

Hydropathy analysis (22) of the deduced amino acid sequence of the AGR1 protein suggested that the region between positions 152 and 502 is hydrophilic, while the N and C termini are hydrophobic and predicted to form a total of 10 transmembrane domains (Fig. 3 *c* and *d*).

Database searches (23) with the AGR1 amino acid sequence identified positive matches, including two hypothetical proteins from *A. thaliana* (accession nos. 2829903 and 2829921, 53 and 47% amino acid sequence identities, respectively), YwkB-homolog protein from *Methanococcus jannaschii* (accession no. F64428, 23% identity), and MdcF protein from *Klebsiella pneumoniae* (accession no. 2240016). The homologous sequences from *A. thaliana* and *M. jannaschii* were identified by genome sequencing projects, and their functions are not known. Furthermore, the 319-aa-long MdcF protein of *K. pneumoniae*, which shares 23% identical and another 21% functionally conserved amino acids with AGR1 over its entire sequence (Fig. 3*e*), was predicted to be a malonate transporter. The MdcF protein was shown to share sequence homologies with a number of transporters (24) and with the hypothetical transmembrane YwkB protein of *Bacillus subtilis* (GenBank accession no. 1176957).

***AGR1*-Expressing *S. cerevisiae* Cells Retain Higher Levels of Preloaded ^{3}H-IAA Than Control Cells.** To test whether the AGR1 protein mediates the efflux of auxin from cells, we tested its ability to promote ^{3}H-IAA release from loaded *S. cerevisiae* cells. Results shown in Fig. 4*a* indicated that *AGR1*-expressing yeast cells retained less radioactivity after a 1-hr washing period than control cells expressing an antisense *AGR1*. Furthermore, *AGR1*-expressing yeast cells were more resistant to 5-fluoro-IAA, a toxic IAA derivative, than control cells (Fig. 4*b*).

***AGR1* Is Expressed in the Distal and Central Elongation Zones of *A. thaliana*.** A combination of Northern blot analysis and *in situ* hybridization experiments were used to define the pattern of *AGR1* expression in *Arabidopsis* seedlings and plants. Fig. 5*a* shows that the *AGR1* gene is expressed specifically in roots of both 7-day-old seedlings and 24-day-old plants (Fig. 5*a*, lanes 1 and 3). No *AGR1* transcripts were detected in hypocotyls and cotyledons of young seedlings (Fig. 5*a*, lane 2) or in rosette leaves, cauline leaves, inflorescence stems, flowers, or siliques of mature plants (Fig. 5*a*, lanes 4–8). On the other hand, *AGR1* transcripts were found in root, hypocotyl, and cotyledon tissues of 5-day-old etiolated seedlings (Fig. 5*a*,

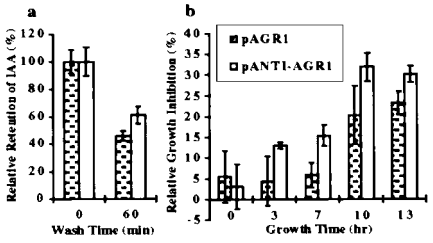

FIG. 4. AGR1 mediates auxin transport in *S. cerevisiae*. (*a*) Relative retention of ^{3}H-IAA by yeast cells transformed with pAGR1 (dotted bar) or with pANTI-AGR1 (open bar), after 0 and 60 min in the wash solution (see *Materials and Methods*). Total number of counts at time 0 (470 cpm for W3031A[pAGR1] and 752 cpm for W3031A[pANTI-AGR1]) are plotted as 100%. Each data point represents an average of two measurements. The vertical bars represent the range of the measurements. (*b*) Relative growth inhibition by 1 mM F-IAA of yeast cells transformed with pAGR1 (dotted bar) or with pANTI-AGR1 (open bar) after 0, 3, 7, 10, and 13 hr of treatment (see *Materials and Methods*). Each point represents an average of three independent measurements. SDs are shown by vertical bars.

lanes 9 and 10). When compared with the expression level of a control *eIF4A* gene, the steady-state level of *AGR1* transcripts was found to be 10 times higher in roots than in hypocotyl and cotyledon tissues of etiolated seedlings (Fig. 5*a*, lanes 9 and 10).

Whole-mount *in situ* hybridization using an antisense *AGR1* RNA probe revealed the existence of *AGR1* transcripts in cells of the distal elongation zone (Fig. 5*b Left*). The hybridization signal intensity decreased from the tip of the root to the mature zone (Fig. 5*b Left*). Control hybridization experiments using either a sense *AGR1* RNA probe on wild-type seedlings (Fig. 5*b Right*) or an antisense *AGR1* RNA probe on *agr1–7* seedlings (data not shown) indicated that the signal found in Fig. 5*b* (*Left*) was *AGR1*-specific.

DISCUSSION

All *agr1* alleles conferred altered root gravitropism, increased root-growth sensitivity to high concentrations of 1-NAA, and decreased root-growth sensitivity to ACC, a precursor of ethylene biosynthesis. Most alleles also conferred a decreased root-growth sensitivity to TIBA, a specific inhibitor of polar auxin transport (Fig. 1). The only exception was *agr1–4*, which exhibited a wild-type response to TIBA (data not shown). This phenotypic difference between *agr1–4* and other *agr1* alleles may reflect functional differences among *agr1* alleles or a difference in phenotypic expression of *agr1* mutations in different ecotype backgrounds.

These phenotypes suggest that *AGR1* plays an important role in the efflux phase of polar auxin transport in roots. Indeed, TIBA is a specific inhibitor of the auxin efflux carrier in plants (2). Furthermore, ethylene is known to promote a reduction in both the abundance of a membrane-associated regulatory subunit of the auxin efflux carrier and the auxin transport activity (2). At the same time, a defect in the auxin efflux carrier is expected to result in an increased sensitivity to auxin, consistent with our observation (Fig. 1*a*). Indeed, mutant root cells are not expected to export as efficiently as wild-type cells an excessive amount of inhibitory auxin taken up from the medium. Interestingly, the latter phenotype is opposite from the phenotype exhibited by *aux1* roots, which carry a defective auxin influx carrier (17).

An involvement of *AGR1* in the efflux phase of polar auxin transport in roots is supported by the fact that preloaded ^{3}H-IAA is retained more efficiently by *agr1* root tips than by wild-type root tips. However, we have not formally excluded possible changes in auxin metabolism or possible differential effects of wounding on ^{3}H-IAA retention by wild-type and mutant root tips (Fig. 1*d*). It is interesting to note that *agr1–5* mutant root tips did not retain more ^{3}H-IAA than wild-type root tips immediately after loading. This surprising result may be explained by the fact that *AGR1* is expressed only in limited and specific regions of the root tips. Alternatively, it is possible that more complex processes feedback-regulate the intake, or modify the transport, of exogenously added auxin in different regions of the root tip.

AGR1 involvement in polar auxin transport is demonstrated by the fact that *AGR1* expression in *S. cerevisiae* results in increased resistance to F-IAA, a toxic IAA-derived compound, and an enhanced cellular efflux of preloaded ^{3}H-IAA (Fig. 4). That model also is in complete agreement with the fact that *AGR1* is expressed in the distal and central elongation zones of *Arabidopsis* root tips (Fig. 5) and encodes a putative transmembrane protein with homologies to bacterial transporters (Fig. 3).

In addition to being specifically expressed in the root distal and central elongation zones of light- and dark-grown seedlings, *AGR1* is also expressed in the hypocotyl and cotyledon tissues of young etiolated seedlings (Fig. 5). The latter observation is not surprising since *agr1* mutations cause a transient randomization of hypocotyl tip angles in etiolated seedlings early after germination (E.R. and Kenneth L. Poff, unpublished results).

While our work was being reviewed, an independent paper (25) reported on the physiological characterization and molecular cloning of *EIR1/AGR1*. Similarly, these authors observed an increased root-growth resistance to ACC and TIBA of *eir1* mutants compared with wild type. However, they reported no differences in root-growth sensitivities to 1-NAA. The inconsistency may result from differences in experimental procedures and/or in alleles tested. Luschnig *et al.* (25) reported that *EIR1*-expressing yeast cells were more resistant to F-IAA and that *eir1* mutations affected the gravitropically regulated *PIG4*::*GUS* reporter gene expression. They concluded that *AGR1* encodes a protein involved in auxin transport in roots. Our *in situ* localization of *AGR1* transcripts in the

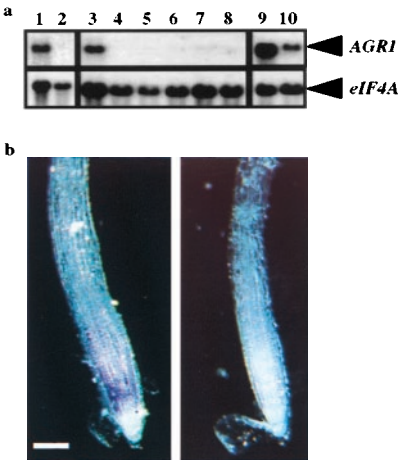

FIG. 5. The pattern of *AGR1* gene expression. (*a*) Northern blot analysis of total RNA extracted from tissues of 7-day-old seedlings (lanes 1 and 2) or 24-day-old (lane 3 to 8) or 5-day-old etiolated (lanes 9 and 10) plants. Tissues from roots (lanes 1, 3, and 9), hypocotyls and cotyledons (lanes 2 and 10), rosette leaves (lane 4), cauline leaves (lane 5), inflorescence stems (lane 6), flowers (lane 7), and siliques (lane 8) were analyzed. A 900-bp cDNA corresponding to the 3′ end of *AGR1* was used as the probe (see *Materials and Methods*). After exposure, the blots were stripped and rehybridized with an *eIF4A* probe to control for loading differences. (*b*) Whole-mount *in situ* hybridization analysis of 3-day-old wild-type root tips, using digoxygenin-labeled antisense (*Left*) and sense (*Right*) RNA probes derived from *in vitro* transcription of the 900-bp-long *AGR1* cDNA template (see *Materials and Methods*). Photos were taken under a dark-field microscope. (Bar = 150 μm.)

distal and central elongation zones of the root tip (Fig. 5) provides further evidence to support this model. In addition, our direct analysis of ^{3}H-IAA retention in root tips (Fig. 1) and, more importantly, in *AGR1*-expressing yeast cells (Fig. 4) demonstrates that AGR1 is indeed an important component of the auxin efflux carrier in root tips.

Localization of the polar auxin transport machinery in the root distal and central elongation zones is consistent with the fountain model of gravitropism, which hypothesizes that an auxin gradient established by lateral auxin transport across a gravistimulated root cap is transported basipetally to the distal and central elongation zones, where it differentially regulates cellular elongation on opposite flanks (reviewed in ref. 1). It is possible that *AGR1* facilitates the transport of the gradient from the cap to more basal regions of the root. Mutations in *AGR1* would simply affect the maximal flow of auxin from the cap to the distal and central elongation zones. Hence, the auxin flow required on the bottom side of a gravistimulated root would be blocked in *agr1* mutants. This model is in complete agreement with the fact that *agr1* mutations promote an increased root-growth sensitivity to only high concentrations of 1-NAA (Fig. 1*a*). It also predicts that another mechanism, possibly mediated by other members of the *AGR1* gene family, may be responsible for the establishment of an auxin gradient across the root cap in response to gravistimulation.

Alternatively, it is also possible that *AGR1* is more directly involved in creating the functional gradient of auxin across a gravistimulated root tip. AGR1 activity could be directly regulated by gravity signals, promoting a differential flow of auxin on opposite flanks of a gravistimulated root (26). It is worth noting that fast changes in proton fluxes have been detected in proximity of the distal elongation zone in response to gravistimulation (27–29), indicating that this region can quickly respond to changes in root-tip orientation within the gravity field.

Mutations in the *AGR1* gene result in a specific defect in root gravitropism, without dramatic pleiotropic phenotypes. Yet, polar auxin transport has been implicated in the regulation of many aspects of plant development, such as vascular tissue differentiation (30), root hair formation, lateral root initiation (31), pattern formation during embryogenesis (32), and development of inflorescence axes, flowers, and leaves (7). This apparent discrepancy may reflect some genetic redundancies in the control of polar auxin transport in plants. Genetic redundancy may also explain why *AGR1* mutations do not result in complete root-growth resistance to TIBA (Fig. 1*b*). The identification of at least two *A. thaliana AGR1* paralogs and of several *A. thaliana* expressed sequence tags potentially encoding AGR1-like proteins (R.C. and P.H.M., unpublished data) supports this hypothesis. A mutational analysis of these paralogs likely will provide further evidence to support a regulatory role of auxin efflux in the development of auxin gradients along and across plant organs and to define the role of such gradients in the regulation of plant growth and development.

We thank T. Sullivan and M. Bennett for discussions; K. Carroll, W. Alphin, and F. Garlick for assistance; W. Sinclair, A. Trewavas, E. Maher, J. Ecker, and K. Okada for providing *agr1* alleles; N. Fedoroff, P. Green, and C. Kung for providing the *Ds*389-14 and *Ds*392-13 lines, the *eIF4A* probe, and strain W3031A, respectively; and the *Arabidopsis* Biological Resource Center for providing DNA stocks and libraries. This work was supported in part by grants from the National Institutes of Health (R01-GM 48053) and the National Aeronautics and Space Administration (NASA) (NAG5-4596), and by a Packard Fellowship (to P.H.M.). R.C. was supported by NASA Grant NAG5-4596; P.H. was supported by Belgian Fonds National de la Recherche Scientifique and European Molecular Biology Organization fellowships; J.S. was supported by National Science Foundation (NSF)/Department of Energy (DOE)/U.S. Department of Agriculture (USDA) (92-2033) and National Institutes of Health (5-T32-6M07133) grants; and E.R. was supported by a NSF/DOE/USDA grant (92-2033). This is paper no. 3528 of the Laboratory of Genetics.

1. Masson, P. H. (1995) *BioEssays* **17,** 119–127.
2. Lomax, T. L., Muday, G. K. & Rubery, P. H. (1995) in *Plant Hormones-Physiology, Biochemistry, and Molecular Biology*, ed. Davies, P. J. (Kluwer, Dordrecht, The Netherlands), pp. 509–530.
3. Bell, C. J. & Maher, E. P. (1990) *Mol. Gen. Genet.* **220,** 289–293.
4. Okada, K. & Shimura, Y. (1990) *Science* **250,** 274–276.
5. Roman, G., Lubarsky, B., Kieber, J. J., Rothenburg, M. & Ecker, J. R. (1995) *Genetics* **139,** 1393–1409.
6. Rutherford, R. & Masson, P. (1996) *Plant Physiol.* **111,** 987–998.
7. Okada, K., Ueda, J., Komaki, M. K., Bell, C. J. & Shimura, Y. (1991) *Plant Cell* **3,** 677–684.
8. Garbers, C., DeLong, A., Deruere, J., Bernasconi, P. & Soll, D. (1996) *EMBO J.* **15,** 2115–2124.
9. Michelmore, R. W., Paran, I. & Kesseli, R. V. (1991) *Proc. Natl. Acad. Sci. USA* **88,** 9828–9832.
10. Bell, C. J. & Ecker, J. R. (1994) *Genomics* **19,** 137–144.
11. Konieczny, A. & Ausubel, F. M. (1993) *Plant J.* **4,** 403–410.
12. Smith, D., Yanai, Y., Liu, Y. G., Ishiguro, S., Okada, K., Shibata, D., Whittier, R. F. & Fedoroff, N. V. (1996) *Plant J.* **10,** 721–732.
13. Reerie, W. G., Feldmann, K. A. & Marks, M. D. (1992) *Genes Dev.* **8,** 1388–1399.
14. Schulz, B., Bennett, M. J., Dilkes, B. P. & Feldmann, K. A. (1994) in *Plant Molecular Biology K3* (Kluwer, Dordrecht, the Netherlands).
15. Schmidt, R., Love, K., West, J., Lenehan, Z. & Dean, C. (1997) *Plant J.* **11,** 563–572.
16. Ausubel, F. M., Brent, R., Kingston, R. E., Moore, D. D., Seidman, J. G., Smith, J. A. & Struhl, K. (1994) *Current Protocols in Molecular Biology* (Wiley, New York).
17. Bennett, M. J., Marchant, A., Green, H. G., May, S. T., Ward, S. P., Millner, P. A., Walker, A. R., Schulz, B. & Feldmann, K. A. (1996) *Science* **273,** 948–950.
18. Newman, T., deBruijn, F. J., Green, P., Keegstra, K., Kende, H., McIntosh, L., Ohlrogge, J., Raikhel, N., Somerville, S., Thomashow, M., *et al.* (1994) *Plant Physiol.* **106,** 1241–1255.
19. Mumberg, D., Mueller, R. & Funk, M. (1994) *Nucleic Acids Res.* **22,** 5767–5768.
20. Chang, C., Bowman, J. L., DeJohn, A. W., Lander, E. S. & Meyerowitz, E. M. (1988) *Proc. Natl. Acad. Sci. USA* **85,** 6856–6860.
21. Hebsgaard, S. M., Korning, P. G., Tolstrup, N., Engelbrecht, J., Rouze, P. & Brunak, S. (1996) *Nucleic Acids Res.* **24,** 3439–3452.
22. Hofmann, K. & Stoffel, W. (1993) *Biol. Chem. Hoppe-Seyler* **347,** 166.
23. Altschul, S. F., Madden, T. L., Schaffer, A. A., Zhang, J., Zhang, J., Miller, W. & Lipman, D. J. (1997) *Nucleic Acids Res.* **25,** 3389–3402.
24. Hoenke, S., Schmid, M. & Dimroth, P. (1997) *Eur. J. Biochem.* **246,** 530–538.
25. Luschnig, C., Gaxiola, R. A., Grisafi, P. & Fink, G. R. (1998) *Genes Dev.* **12,** 2175–2187.
26. Sachs, T. (1981) *Adv. Bot. Res.* **9,** 152–265.
27. Mulkey, T. J. & Evans, M. L. (1981) *Science* **212,** 70–71.
28. Bjokmann, T. & Leopold, A. C. (1987) *Plant Physiol.* **83,** 841–846.
29. Zieschang, H. E., Köhler, K. & Sievers, A. (1993) *Planta* **190,** 546–554.
30. Hardtke, C. S. & Berleth, T. (1998) *EMBO J.* **17,** 1405–1411.
31. Celenza, J. L. J., Grisafi, P. L. & Fink, G. R. (1995) *Genes Dev.* **9,** 2131–2142.
32. Hadfi, K., Speth, V. & Neuhaus, G. (1998) *Development* (Cambridge, U.K.) **125,** 879–887.